# Experimental study on cross-sensitivity of temperature and vibration of embedded fiber Bragg grating sensors*

**CHEN Tao** (陈涛), **YE Meng-li** (叶梦力)**, **LIU Shu-liang** (刘树良), **and DENG Yan** (邓炎)
*School of Mechanical and Electronic Engineering, Wuhan University of Technology, Wuhan 430070, China*

(Received 23 October 2017; Revised 16 November 2017)


In view of the principle for occurrence of cross-sensitivity, a series of calibration experiments are carried out to solve the cross-sensitivity problem of embedded fiber Bragg gratings (FBGs) using the reference grating method. Moreover, an ultrasonic-vibration-assisted grinding (UVAG) model is established, and finite element analysis (FEA) is carried out under the monitoring environment of embedded temperature measurement system. In addition, the related temperature acquisition tests are set in accordance with requirements of the reference grating method. Finally, comparative analyses of the simulation and experimental results are performed, and it may be concluded that the reference grating method may be utilized to effectively solve the cross-sensitivity of embedded FBGs.
**Document code:** A **Article ID:** 1673-1905(2018)02-0092-6
**DOI** https://doi.org/10.1007/s11801-018-7228-5

Fiber Bragg grating (FBG) temperature sensors, as a kind of excellent sensing measurement devices, have many advantages, such as high sensitivity, small volume and mass, easily bending, anti-electromagnetic interference and good corrosion resistance, so that it may be popular in various temperature monitoring conditions in many industries. The ultrasonic-vibration-assisted grinding (UVAG) is an effective method for processing carbon fiber reinforced plastics (CFRP), for which the grinding temperature shall be controlled strictly to improve the surface quality of workpieces. However, intensive vibration occurs due to the inverse piezoelectric effect during its manufacturing processes, which may changes the center wavelength of the FBG to a certain extent. Moreover, those physical quantities leading to the change of center wavelength at the same time may not be recognized by a single FBG while it is affected due to not only temperature but also strain. Thus, the cross-sensitivity of FBGs occurs to seriously restrict the detection of grinding temperature for CFRP under UVAG situation[1-3].

Further comprehensive studies about the cross-sensitivity of FBGs have been carried out by some scholars in recent years. Liang et al[4] designed a scheme applicable for solving the cross-sensitivity of stress and temperature for sensing measurement of temperature by means of FBGs with a long period, which is based on the concept of relation for converting the negative interference of strain on temperature into the correspondingly positive sensitization effect, so that the cross-sensitivity of FBG temperature sensors with a long period may be better solved. Zhang et al[5] put forward a scheme which includes a spring being equipped in a metal tube for pre-stressed encapsulation to solve the cross-sensitivity, and the experimental verification was carried out to indicate that the sensor has good linearity and repeatability for achievement of accurate measurement of temperature. Han et al[6] defined the correlation function between tensile force and temperature to separate the temperature factor out of the cross relationship between wavelength and temperature or tensile force, and the theoretical study was carried out to the relevant characteristics between tensile force and temperature of FBGs, so that the measured data may indicate better solution of the cross-sensitivity between temperature and tensile force. Korenko et al[7] designed a device encapsulated by means of ormocer for thermal compensation of FBGs to effectively achieve robust measurement of the cross-sensitivity. Peng et al[8] showed a self-demodulation FBG sensing device so that the cross-sensitivity of FBGs may be solved by means of propagation of various signals.

In case of the inevitable cross-sensitivity in actual measurement process, those solutions, such as the reference grating, double grating, double-parameter and temperature (or strain) compensation methods, generally may be put into operation to improve the measurement accuracy[9,10]. As for the reference grating method, the strain (or temperature) is measured by an FBG sensor, and the temperature (or strain) is measured by means of the other FBG sensor at the same time, the both drifts of the Bragg wavelength may be processed to solve the change due to a single parameter, thus, the cross-sensitivity may

* This work has been supported by the Science and Technology Department of Hubei Province in China (No.2015BAA022).
** E-mail: 952297563@qq.com

be solved. Only two FBGs may be necessary for such methods so that it shall be simple and practicable, and a better desensitization effect may be achieved by designing a proper arrangement scheme.

In view of those basic requirements of monitoring temperature of CFRP under UVAG situation, an embedded FBGs temperature measurement system is designed to improve the accuracy of data acquisition for the temperature measurement system. Firstly, the theoretical analysis is performed to the cross-sensitivity of FBGs. Secondly, a series of calibration experiments are carried out for description of the embedded FBGs temperature measurement system, which may conform to those basic conditions by means of the reference grating method to solve the cross-sensitivity of FBGs. Finally, the comparative analysis (about whether it has consistency in a certain range) is carried out through the results of experiments and simulations to verify the feasibility of the reference grating method to solve the cross-sensitivity of FBGs.

Fig.1 shows the structure of an FBG sensor. When the FBG is illuminated with broadband light, the grating is equivalent to a narrow bandwidth optical mirror in optical fiber, which selectively reflects a part of incident light, whose wavelength conforms to the Bragg phase matching conditions, and the other part of incident light in other wavelengths is in the transmission mode. The Bragg equation of FBG is listed as follows based on the above principle[11-13]:

$$\lambda_B=2n_{eff}\cdot\Lambda, \tag{1}$$

where $\lambda_B$ represents the center wavelength of the FBG, $n_{eff}$ represents the effective refractive index of the FBG, and $\Lambda$ represents the period of the FBG.

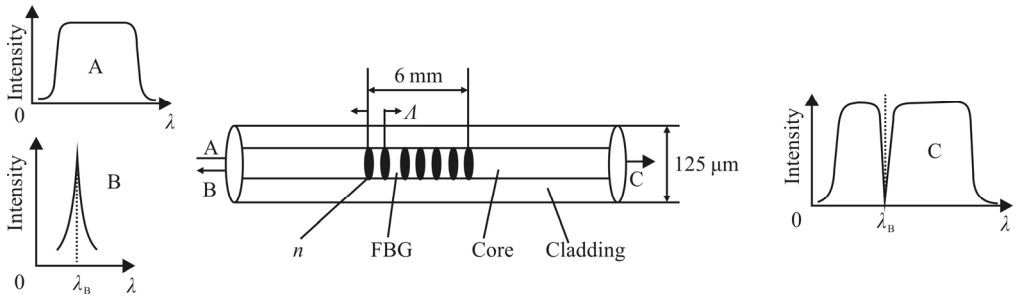


**Fig.1 The operating principle of an FBG sensor, where A is the input spectrum, B is the reflected signal, and C is the transmitted signal**

While an FBG sensor is only under stress, the corresponding strain occurs so that the fiber grating period may change. Moreover, the changing refractive index of the FBG leads to the change of $\lambda_B$, which may be expressed based on Eq.(1) as

$$\Delta\lambda_B=K_\varepsilon\cdot\Delta\varepsilon, \tag{2}$$

where $\Delta\varepsilon$ represents the strain of the FBG, $K_\varepsilon=\lambda_B(1-p_e)$ represents the strain sensitivity coefficient of the FBG, which is a constant and only related to material properties of the FBG, and $p_e$ represents the elasto-optical coefficient of optical fiber.

On the other hand, while an FBG sensor is only under temperature, its grating period and refractive index may also change. The change of $\lambda_B$ may also be expressed based on Eq.(1) as

$$\Delta\lambda_B=K_T\cdot\Delta T, \tag{3}$$

where $\Delta T$ represents the temperature variation, $K_T=\lambda_B(\alpha+\zeta)$ represents the temperature sensitivity coefficient of the FBG sensor, which is a constant and only related to material properties of the FBG sensor, $\alpha$ represents the thermal expansion coefficient of optical fiber, and $\zeta$ represents the thermo-optical coefficient of optical fiber.

The center wavelength of FBG sensor may be affected simultaneously by strain and temperature in any actual measurement process. Moreover, those sources for changing its center wavelength may not be recognized by means of a single FBG so that the cross-sensitivity of FBG may occur. Eq.(1) may indicate that $n_{eff}$ and $\Lambda$ are related to $\Delta\lambda_B$. Taylor series expansion of Eq. (1) leads to the following equations:

$$\Delta\lambda_B=\Delta\varepsilon\left[\frac{\partial\lambda_B}{\partial\varepsilon}\right]+\Delta T\left[\frac{\partial\lambda_B}{\partial T}\right]+\Delta\varepsilon\Delta T\left[\frac{\partial^2\lambda_B}{\partial\varepsilon\partial T}\right]+\frac{1}{2!}\left\{(\Delta\varepsilon)^2\left[\frac{\partial^2\lambda_B}{\partial\varepsilon^2}\right]+(\Delta T)^2\left[\frac{\partial^2\lambda_B}{\partial T^2}\right]\right\}+\cdots, \tag{4}$$

$$K_\varepsilon=\lambda_B(1-p_e)=\left[\frac{\partial\lambda_B}{\partial\varepsilon}\right], \tag{5}$$

$$K_T=\lambda_B(\alpha+\zeta)=\left[\frac{\partial\lambda_B}{\partial T}\right]. \tag{6}$$

Eq.(4) indicates that $\Delta\lambda_B$ is related to $\Delta\varepsilon$, $\Delta T$ and their cross and higher-order terms, whereas, those cross and higher-order terms may be negligible while temperature and strain of the FBG are within relatively small ranges ($\Delta t\leq150$ °C, $\Delta\varepsilon\leq5$ nm). Thus, the following equation may be obtained under general measurement situations:

$$\Delta\lambda_B=K_\varepsilon\cdot\Delta\varepsilon+K_T\cdot\Delta T. \tag{7}$$

The above relation reflects the basic equation of principle for occurrence of the cross-sensitivity of FBGs, from which it may be seen that $\Delta T$ and $\Delta\varepsilon$ may independently affect $\lambda_B$, respectively, and the both effects may be linearly superposed, so the corresponding drifts

of the Bragg wavelength may not be recognized by means of a single FBG or the accurate decomposed results may not be got while $\Delta T$ and $\Delta\varepsilon$ simultaneously change in a measurement point.

Finite element simulation was carried out by means of ANSYS software after establishing the model shown in Fig.2.

The embedded FBGs temperature measurement system includes FBG1 for temperature measurement and FBG2 for vibration measurement, whose arrangement schematic diagram is shown in Fig.2. FBG1 are arranged in three positions surrounding the processing region for comprehensively monitoring the temperature distribution of the grinding region, whose specific location inside the workpiece is shown in Fig.2, where $d$ represents the diameter of the diamond grinding head, and $a_p$ represents the grinding depth. FBG2 is far away from the grinding region, and the distance between the location of FBG2 and the grinding region is defined as the thermal insulation distance which may be obtained by means of the simulation cloud picture shown in Fig.3 to ensure FBG2 shall be free of interference of the grinding temperature. The sensing elements of FBG1 and FBG2 are located at the middle place of the four holes along the FBGs[14,15].

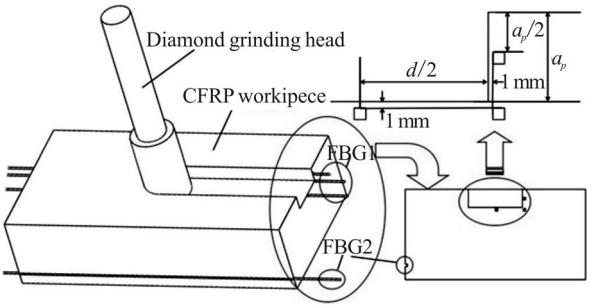


**Fig.2 Arrangement schematic diagram of FBGs**

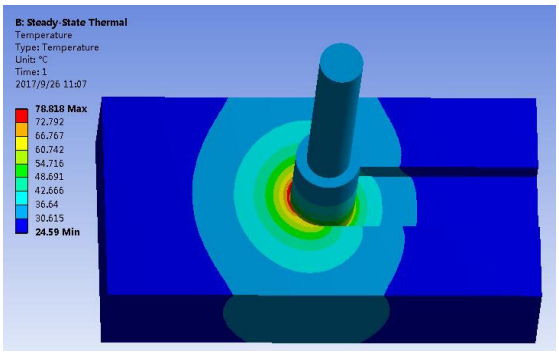


**Fig.3 Temperature cloud picture**

The thickness of a layer of the CFRP workpiece is 0.263 mm, and the diameter of each FBG is 0.125 mm.

The specific FBGs arrangement holes were left during the multi-layer pressing formation process for placement of FBG1 and FBG2 (Fig.4). Due to FBG2 being in the edge of the workpiece as shown in Fig.2, the design scheme for placement of FBG2 is equivalent to the scheme in Fig.4 without part 1, so that layer 2 shall only include part 2 and the hole. FBG1 and FBG2 are directly placed inside the arrangement holes fully coated with thermally conductive silicone grease and thermal insulation glue to prevent any temperature interference, respectively, and the thermal insulation effect will be experimentally verified subsequently.

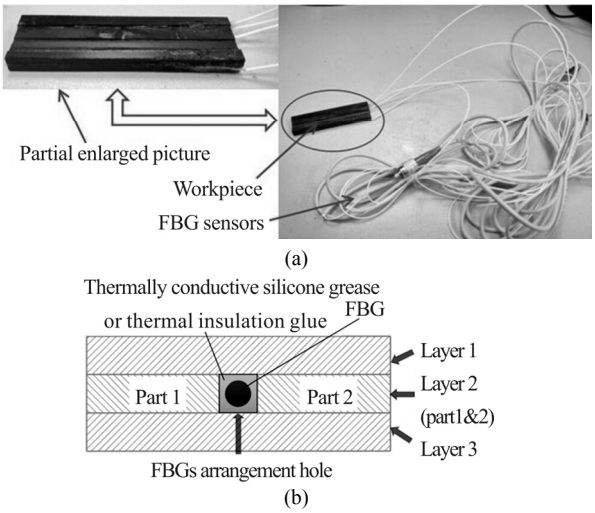


**Fig.4 (a) Photo and (b) formation of FBGs in the multi-layer workpiece**

The experimental setup shown in Fig.5 includes a computerized numerical control machining center (CNC), a UVAG device and an FBG temperature measurement system (FBG1 and FBG2). As for FBGs, their wavebands are both within 1 540—1 550 nm, and their metallized surfaces are electroplating copper sulfate for encapsulation of optical fiber process. The parameters of FBGs (FBG1 and FBG2) are all the same except center wavelength as shown in Tab.1.

First of all, FBGs shall be selected based on calibration experiments, during which temperature and vibration calibration would be carried on 20 FBGs. Secondly, the data acquisition was carried out for MATLAB fitting analysis. Finally, 4 FBGs were selected for subsequent experiments, and their corresponding curve-fitting equations are fully the same (the decimal digits of various coefficients are 4), whose tolerance ranges conform to the operation requirements of the reference grating method.

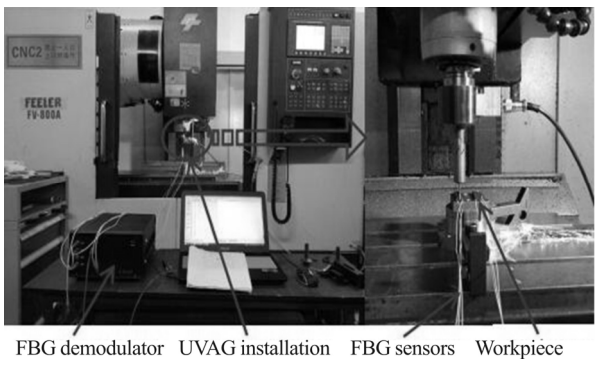


**Fig.5 Picture of experimental setup**

**Tab.1 Material properties of FBGs**

| Parameter | Value |
|---|---|
| Center wavelength | 1 540—1 550 nm |
| Reflectivity | ≥90% |
| Side-length suppression ratio | ≥13 dB |
| 3 dB bandwidth | ≤0.25 nm |
| Wavelength error | ±0.2 nm |
| Grating length | 6 mm |
| Core diameter | 0.125 mm |
| Grating point | 12 |
| Tail fiber length | 1/1 m |
| Cladding material | Acrylate |
| Minimum bending radius | 2 mm |

While a CFRP workpiece is processed by means of the UVAG, the grinding temperature of the region in contact with the tool is maximum so that this temperature may gradually fall due to transferring heat to the surrounding areas. Thus, the final grinding temperature shall be selected as the maximum among the measured temperatures of 3 FBGs at the same time to ensure that data for analysis shall be the most closest to the temperature of the actually grinding region.

As for temperature calibration, a 3-hole electric thermostatic water bath with temperature control range of 5—100°C, and temperature resolution of 0.1°C was utilized to control the temperature and conform to the temperature control requirements of experiments, as shown in Fig.6. The calibration temperature range is 25—100 °C, and the temperature interval is 0.1 °C. There are 760 sampling points in total, and the corresponding fitting curves were derived by fitting these sampling points in MATLAB software. Moreover, the above tests were carried out again to demonstrate the good repeatability of this type of sensors. Finally, 2 groups of measured results are expressed in Fig.7 (FBG1) and Fig.8 (FBG2), which may indicate that the $R^2$ values of FBG1 and FBG2 are above 0.999 5, and the good repeatability is reflected for the two temperature calibration experiments. Thus, the FBG1 (FBG2) temperature sensor has good comprehensive performances to conform to the experimental requirements.

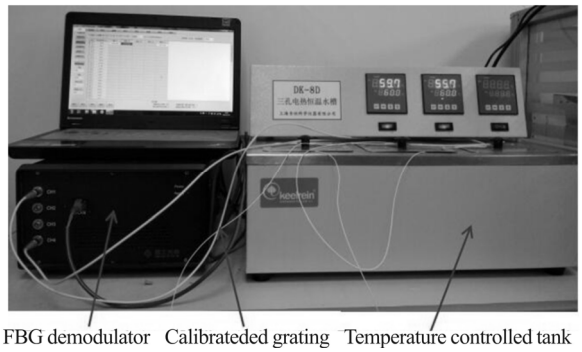


**Fig.6 Experimental setup picture for temperature calibration**

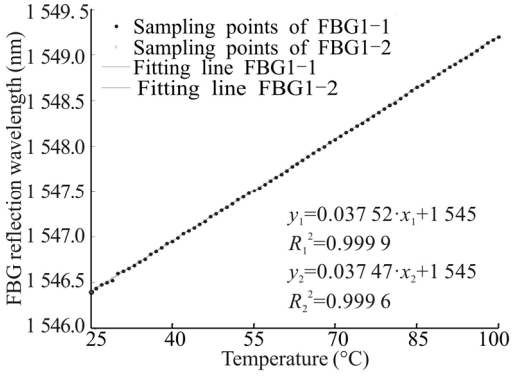


**Fig.7 Fitting curves and equations for temperature calibration of FBG1**

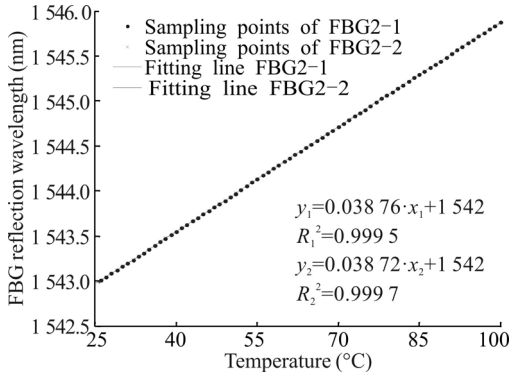


**Fig.8 Fitting curves and equations for temperature calibration of FBG2**

As for vibration calibration of FBG2, a strong electric type small vibrator with frequency range of 10—2 000 Hz, output power of 1 500 W, including shaker table, power amplifier and signal generator, were utilized. During the experimental processes, the frequency range is 200—2 000 Hz, and the sampling frequency interval is 50 Hz. There are 37 sampling points in total. In addition, 2 groups of measured results are expressed in Fig.10, which may indicate that the $R^2$ values of FBG2 are above 0.999 5, and the good repeatability is reflected for the two vibration calibration experiments. Thus, the FBG2 has good comprehensive performances to conform to the experimental requirements.

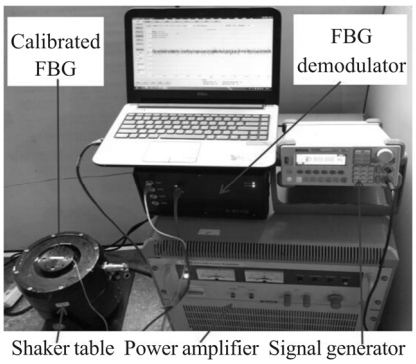


**Fig.9 Experimental setup picture for vibration calibration of FBG2**

The following issues are solved in the calibration of FBG2.

1) For ensuring the stability of corresponding center wavelength, all center wavelength values recorded by the system within 5 s are acquired at the same vibration frequency, and then they are averaged as the corresponding center wavelength at this frequency.

2) As FBG1 for the temperature measurement is equipped in various locations, and the synchronism of their vibration responses shall be verified. Moreover, it shall be verified whether their response ranges (or wavelength change ranges) are the same. Successful solution of the cross-sensitivity by means of FBG2 depends on solution of this issue. Thus, experimental verification is carried out to this issue during the calibration experiments. FBG2 is calibrated while it is located in four different positions as shown in Fig.2 for placement of FBG2 sensors, whose fitting curves are presented in Fig.10, and it is indicated that the $R^2$ values for calibration of FBG2 in four positions are above 0.999 5 and their corresponding fitting curves also reflect the good repeatability of FBG2 so as to demonstrate the responses of FBG2 in four positions are synchronous and the corresponding response ranges (or wavelength change ranges) are the same. Thus, the layout method of FBG2 may be utilized to solve the cross-sensitivity.

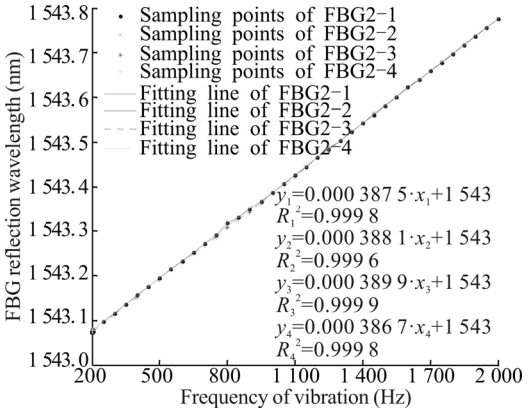


**Fig.10 Fitting curves and equations for vibration calibration of FBG2 in various locations**

3) While FBG2 is arranged in the specific mounting groove coated fully with the thermal insulation glue, FBG2 is fixed firmly in the workpiece. Besides, the thermal insulation glue may contribute to the elimination of effect of grinding temperature to the reflection wavelength of FBG2. For verification of the feasibility of such a method, calibration experiments are carried out after placing FBG2 and coating the thermal insulation glue in those environments (only vibration and vibration & temperature), in which the temperature at the location of FBG2 may be roughly measured by means of a pyrometer, and a moving heat source was utilized to achieve the temperature above the UVAG temperature. The corresponding measured results shown in Fig.11 indicate that the $R^2$ values for calibration of FBG2 in the both situations are above 0.9995, and their corresponding fitting curves also reflect the good repeatability of FBG2 and the good thermal insulation performance of the glue.

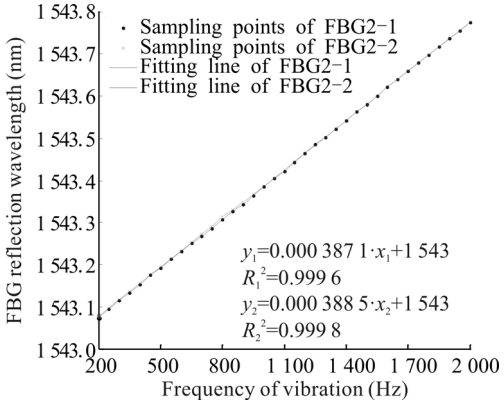


**Fig.11 Fitting curves and equations for vibration calibration of FBG2 for the verification of effect of the thermal insulation glue**

Those grinding parameters in Tab.2 are utilized to process CFRP workpieces, and the measurement data related to the grinding temperature of FBGs are also recorded in Tab.2. As for measurement of the grinding temperature, firstly, the wavelengths under the temperature & vibration effects are got by FBG1, and the wavelengths under the vibration effect only are obtained by FBG2. Secondly, the drifts of the center wavelength of FBG1 and FBG2 are derived based on the comparison with the corresponding center wavelength values in Tab.1. Thirdly, the center wavelength drifts only due to the grinding temperature may be gained based on the differences between the center wavelength drifts of FBG1 and FBG2. Finally, the relationships between the drift magnitude of central wavelength and the temperature in calibration of FBG1 are shown in Fig.12 for contrast analysis so that the actual grinding temperature may be obtained. The above data related to any center wavelength drift are reflected in Tab.2.

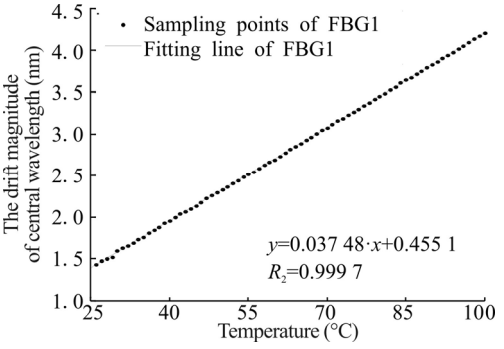


**Fig.12 The relationship between the drift magnitude of central wavelength and the temperature**

It may be indicated based on comparison of the

simulated grinding temperature values and the actual temperature values measured by means of FBGs under the same processing conditions, which are shown in Tab.2, that the both groups of temperature data change in the consistent trends and their differences are among the range (2—4°C). Thus, the grinding temperature may be measured accurately by means of such a method, that is to say, the reference grating method may be an successful solution of the cross-sensitivity of FBG temperature sensors.

**Tab.2 Temperature measurement and simulated data of FBGs**

| Experiment | Spindle speed (r/min) | Feed rate (mm/min) | Cutting depth (mm) | Drift of center wavelength of FBG1 (nm) | Drift of center wavelength of FBG2 (nm) | Actual drift of center wavelength for temperature measurement (nm) | Simulated temperature (°C) | Actual grinding temperature (°C) |
|---|---|---|---|---|---|---|---|---|
| 1 | 500 | 100 | 0.1 | 1.409 4 | 0.273 2 | 1.136 2 | 21 | 18 |
| 2 | 1 000 | 140 | 0.15 | 1.839 6 | 0.362 8 | 1.476 8 | 29 | 27 |
| 3 | 1 500 | 180 | 0.2 | 2.516 0 | 0.547 3 | 1.968 7 | 44 | 40 |
| 4 | 2 000 | 220 | 0.25 | 3.537 2 | 0.698 2 | 2.839 0 | 65 | 63 |
| 5 | 2 500 | 260 | 0.3 | 4.608 5 | 0.785 6 | 3.822 9 | 93 | 89 |

The embedded FBGs temperature measurement system can be actually applied to accurately and real-time monitor the grinding temperature of any CFRP workpiece during UVAG processes by means of the simulation and grinding experiments, and provide a reliable temperature monitoring scheme for study of the related research in future.

From the theoretical analysis of the cross-sensitivity of FBGs, a series of calibration experiments were carried out to demonstrate the embedded FBGs temperature measurement system, which may conform to those basic conditions for solution of the cross-sensitivity of FBGs by means of the reference grating method. Finally, the comprehensive analyses of the measured and simulated results were carried out to verify the feasibility of solution of the cross-sensitivity of FBGs by means of the reference grating method.

Study on the cross-sensitivity of FBGs has been remaining primarily in the theoretical level, and several corresponding solutions were put forward at home and abroad in recent years. However, little related research was reported about verification of various solutions in the experimental level. The reference grating method was focused in this study to perform contrastive analysis of its advantages in theory and verify its practicability based on the simulation and experimental analysis. Finally, it is deduced that the reference grating method may be utilized to solve the cross-sensitivity. The experiments are based on CFRP workpieces under the UVAG processes, and the scheme for layout of temperature and vibration measurement FBGs is designed. Moreover, analyses are carried out by taking an actual case including the cross-sensitivity due to the ultrasonic vibration in temperature measurement experiments. Thus, the cross-sensitivity and accuracy due to the temperature measurement are solved. In addition, the reliability of reference grating method is verified to solve actual issues.

## References


[1] Liu Shu-liang, Chen Tao and Wu Chao-qun, International Journal of Advanced Manufacturing Technology **89**, 847 (2017).

[2] Sengupta S, Ghorai S-K and Biswas P, IEEE Sensors Journal **16**, 7941 (2016).

[3] Marzbanrad B, Jahed H and Toyserkani E, Journal of Advanced Manufacturing Technology **86**, 3453 (2016).

[4] Liang Li-li, Liu Ming-sheng, Li Yan, Li Yu-guo and Yang Kang, Infrared and Laser Engineering **44**, 1020 (2015). (in Chinese)

[5] Zhang Deng-pan, Zheng Yan, Wang Jin and Wang Yong-jie, Journal of Atmospheric & Environmental Optics **11**, 226 (2016). (in Chinese)

[6] Han Gui-hua, Liu Yan-wei and Chen Jiu-ju, Journal of Heilongjiang Institute of Technology 26, **38** (2012). (in Chinese)

[7] Branislav K, Manfred R, Alexander H and Hartmut B, IEEE Sensor Journal **15**, 5450 (2015).

[8] Peng Bao-jin, Zhao Yong, Zhao Yan and Yang Jian, IEEE Sensor Journal **6**, 63 (2006).

[9] Ghafarizadeh S, Chatelain J-F and Lebrun G, International Journal of Advanced Manufacturing Technology 87, **399** (2016).

[10] Chen Tao, Ye Meng-li, Liu Shu-liang and Tian Shen-ling, International Journal of Advanced Manufacturing Technology **93**, 2561 (2017).

[11] Li Shuo, Huang Jun-bin, Gu Hong-can, Sun Jin-wei and Yang Guang, Ship Science and Technology **34**, 77 (2012). (in Chinese)

[12] Wee J, Hackney D, Bradford P and Peters K, Journal of Lightwave Technology **PP**, 1 (2017).

[13] Mamidi V-R, Kamineni S and Ravinuthala Lnsp, Fiber & Integrated Optics **33**, 325 (2014).

[14] Kaur G, Kaler R-S and Kwatra N, Optik-International Journal for Light and Electron Optics**131**, 483 (2017).

[15] Li Tian-liang, Tan Yue-gang, Wei Li, Zhou Zu-de, Zheng Kai and Guo Yong-xiang, Review of Scientific Instruments **85**, 015002 (2014).